# HIGH CURRENT HIGH CHARGE MAGNETIZED AND BUNCHED ELECTRON BEAM FROM A DC PHOTOGUN FOR JLEIC COOLER*

P. Adderley, J. Benesch, D. Bullard, J. Grames, J. Guo, F. Hannon, J. Hansknecht, C. Hernandez-Garcia, R. Kazimi, G. Krafft[1], M. A. Mamun, M. Poelker, R. Suleiman, M. Tiefenback, Y. Wang[1], S. Zhang[†], Thomas Jefferson National Accelerator Facility, Newport News, VA-23606, USA
J. Delayen, S. Wijethunga, Old Dominion University, Norfolk, VA 23529, USA
[1]also at Old Dominion University, Norfolk, VA 23529, USA

## Abstract

A high current, high charge magnetized electron beamline was developed for fast and efficient cooling of ion beams for the proposed Jefferson Lab Electron Ion Collider (JLEIC). In this paper, we describe recent achievements that include the generation of picosecond-bunch magnetized beams at average currents up to 28 mA with exceptionally long photocathode lifetime, and independent demonstrations of magnetized beam with high bunch charge up to 700 pC at 10s of kHz repetition rates. In addition, a detailed description of an extremely stable and reliable fiber-based drive laser system that employs a gain-switched master oscillator is presented. These accomplishments mark important steps toward demonstrating the feasibility of a technically challenging JLEIC cooler design using magnetized beams

## INTRODUCTION

Strong cooling of ion beams is an essential feature for the proposed electron-ion colliders (EIC) to achieve the desired $10^{33}$–$10^{34}$ cm$^{-2}$sec$^{-1}$ luminosity [1-4]. Hadron cooling for both Brookhaven National Laboratory (BNL) and Thomas Jefferson National Accelerator Facility (JLab) requires a very high average current unpolarized high bunch charge electron beam with low emittance and long lifetime. For JLEIC, fast cooling of ion beams will be accomplished via magnetized electron cooling technique using a recirculator ring that employs an energy recovery linac (ERL).

In this work, we report generation of magnetized electron beams from a 300 kV DC high voltage photogun with an inverted insulator geometry. Emittance contribution from beam magnetization was assessed and characterized as a function of applied magnetic field and different laser spot sizes on photocathode. The experimental results are compared with simulations. Lifetime of bialkali antimonide photocathode deposited on molybdenum substrate was assessed at 28 mA over 2 days. In addition, high repetition rate high bunch charge magnetized beams were also produced and studied.
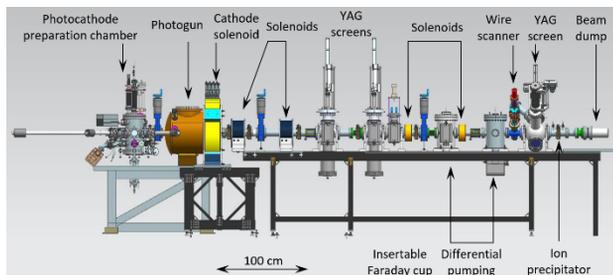
Figure 1: Illustration of main components of the magnetized electron beamline.

## BEAMLINE

The magnetized electron source consists of drive laser system, bialkali-antimonide photocathode, gun HV chamber, gun solenoid, and beamline with diagnostics (Fig. 1), as described in detail in the following sections.

## Drive Lasers

There were two distinctively different drive lasers used for the tests described here. For high current generation, a master-oscillator-power-amplifier system, composed of a 1.066 μm gain-switched diode laser (GSDL) and multistage Yb-fiber amplifier chain followed by a harmonic converter, was constructed to provide Watts of power with picosecond light pulses at 533 nm. The laser system exhibits features that are highly desirable for photocathode-based electron accelerator applications such as adjustable pulse repetition rates from 10s of MHz to a few GHz, variable pulse width from 10s to 100s of picoseconds, and direct synchronization to an external RF signal without requiring rf-laser phase locking systems. Good harmonic conversion efficiency up to 30% was achieved using a PPLN crystal. The sub-mW picosecond seed pulses from the GSDL were amplified to up to 8W using two single mode Yb polarization maintaining (PM) fiber amplifiers and a highly-doped double-clad Yb fiber power amplifier. This laser system operated for months without intervention until key parameter changes were required.

The second laser is a commercial ultrafast laser with pulse duration less than 0.5 ps, 20 μJ pulse energy, operating at 50 kHz pulse repetition and 1030 nm wavelength (NKT Origami). The IR beam was converted to 515 nm using a BBO crystal. To meet the pulse length requirement, a pulse stretcher consisting of a pair of diffraction gratings and reflectors in a double pass configuration was built. The sub-picosecond pulses were lengthened to val-

ues between 75 - 120 ps (FWHM) by changing the dispersion length of the stretcher.

An image-relaying optical transport was shared by both lasers to deliver the light beams from the drive laser enclosure to an optical diagnostic hutch before reaching the photogun chamber. The combination of a Pockel's cell, a waveplate and a mechanical shutter allows electron beam operation in a low duty-factor mode needed for initial machine setup.

### Photocathode Preparation Chamber

Bialkali-antimonide photocathodes were grown inside a preparation chamber using co-evaporation of Cs and K onto a thin Sb layer deposited on a diamond paste polished molybdenum substrate. The substrate was heat cleaned at ~ 700°C for ~ 20 h prior to activation. The technical details of key components of the deposition system and process are similar to [5] and include: i) residual gas analyser to continuously monitor the vacuum gas composition and the deposition chemical species, ii) pure elemental sources of Sb, Cs, and K, iii) two resistive heaters attached to long stalks and mounted on linear translation stages, one at the bottom and another on the top of the chamber, iv) magnetic manipulators to manouver and store the photocathode pucks, and v) NEG and ion pumps for maintaining high vacuum ~ $9 \times 10^{-10}$ Pa following a 100 hrs long bake at 190°C. During chemical deposition the substrate temperature was maintained at ~ 120 °C and the substrate was kept at 3 cm distance from the evaporation sources. The photocurrent was continuously monitored during alkali deposition by applying a low voltage bias (-280 V) and using a 532 nm laser. The photocathode was activated in a two-step process where a thin Sb film deposition was followed by simultaneous deposition of alkalis from an effusion source. The Sb source was resistively heated and the Sb was deposited for 10 minutes to get a translucent Sb layer. A mask with 5 mm aperture was used to limit the photocathode active area within the 13 mm diameter molybdenum substrate. Alkali deposition was discontinued when the photoemission current reached a maximum showing a QE of ~ 5.5 % or higher.

### High Voltage DC Photogun

The photogun is based on a conical inverted geometry insulator designed for operation at -350 kV with maximum gradient of 10 MV/m. This design provides a small volume resulting in better vacuum; the insulator serves as the electrode support structure leaving less metal biased at high voltage contributing to field emission, and lastly high voltage is applied to the cathode electrode using a commercial HV cable with a termination designed to mate with the inverted geometry insulator. The wider end of the 17.8 cm long conical ceramic insulator was mounted on top of the photogun high voltage chamber. A 15.2 cm diameter 316L stainless steel spherical shell electrode was attached to the narrow end of the insulator positioning the electrode at the center of the HV chamber. This configuration permits loading photocathodes into the electrode

using a long manipulator from the preparation chamber via a gate valve. The spherical cathode includes a specially designed screening electrode that reduces the field strength at the triple-point-junction where arcing is thought to originate [6]. The spherical and screening electrodes were barrel polished to achieve a mirror-like surface finish [7]. The drive laser beam passes through entrance and exit holes in the anode electrode at 25° angle of incidence. The anode positioned 9 cm from the photocathode is also electrically isolated from ground potential to enable measurement of field emission from the cathode electrode and to enable biasing as a means to repel downstream ions created by the beam [8]. The photogun was high voltage conditioned to -360 kV using Kr gas to eliminate field emitters [9].

### Cathode Solenoid and Beam Diagnostics

The cathode magnetizing solenoid could provide magnetic field up to 1.5 kG at the photocathode. It was positioned at the front of the gun chamber, 0.2 m away from the photocathode [10, 11]. A procedure was developed and followed during the test to energize cathode solenoid without exciting new field emitters.

The diagnostic consists of: i) three fluorescent YAG screens located at 1.5, 2.0 m, and 3.75 m respectively, ii) seven steering magnets, and iii) four focusing solenoids to compensate space-charge emittance growth and to transport the beam to a Faraday Cup beam dump for photocathode lifetime measurements at milliampere beam current, iv) ion clearing electrode, and v) differential pumps, ion pumps and NEG pumps.
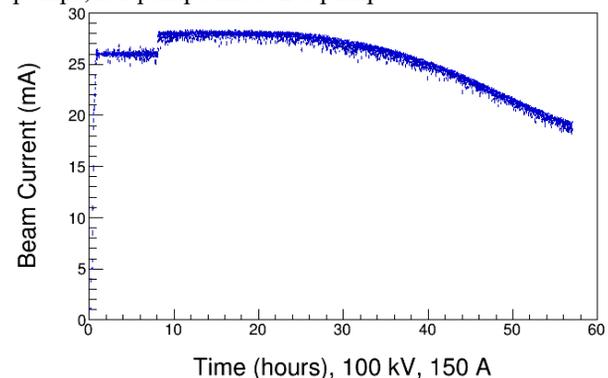


Figure 2: Photocathode QE measured over 2 days with the photogun biased at -100 kV and an initial 28 mA average current. The bias voltage was set to -100 kV for this extended run due to power limit (to 3 kW) of the high voltage power supply.

## RESULTS AND DISCUSSION

High average current and high bunch charge magnetized beams were successfully generated from this beamline. The main results are summarized as follow.

### High Current Beam

Sustained high current beam delivery was achieved by applying a positive bias (+1 kVDC) to the anode. Beamline ion-clearing electrodes [10] were employed to pre-

serve photocathode QE, but alone, these clearing electrodes did not prevent rapid photocathode damage. When the anode is grounded, photocathodes are quickly damaged by "micro-arc discharges" manifested by current spikes, vacuum bursts and subsequent visible damage sites on the photocathode. Figure 2 shows the highest beam current produced at JLab, 28 mA with a cumulative extracted charge of ~5000 C and an estimated 1/e charge lifetime of ~9430 C. A 1.4 mm (rms) laser spot was used with 50 ps (FWHM) pulse width and 374.25 MHz repetition rate. The cathode magnetic field was set at 568 Gauss. The bunch charge of the beam was 75 pC at the dump. The superior thermal conductivity of molybdenum substrate improved charge lifetime over photocathodes grown on GaAs substrate. The photocurrent drop after ~24 hours is likely a result of photocathode heating which indicates the need for cooling for higher current delivery.

### High Bunch Charge Beam

With photogun bias voltage at -225 kV initially, electron beams were extracted from a 1.4 mm (rms) laser spot on the photocathode immersed in a 757 Gauss magnetic field. Beams with 700 pC/bunch were generated and transported to the dump with 75 ps (FWHM) at 50 kHz laser pulses. All of the beamline solenoids were employed in an effort to compensate for the space charge induced emittance growth and to minimize the beam loss on the beamline components with limited aperture.
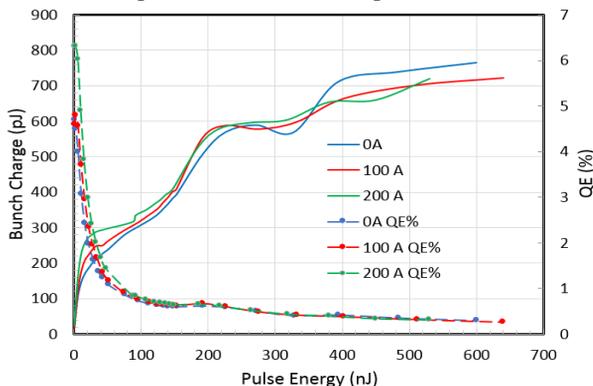
Figure 3: Electron bunch charge and photocathode QE vs. laser pulse energy at two magnet current settings.

Figure 3 presents the variation of extracted charge with the laser pulse energy for different magnet current settings. Traditional Child's Law space charge limitation was observed for bunch charge around 0.3 nC. The additional charge extracted between 0.3 - 0.7 nC was likely a result of beam produced from the edge of the Gaussian laser profile. The beamline vacuum signature during these measurements indicated severe beam scraping occurred. The measured QE falls sharply with laser pulse energy, a clear indication of space charge limitations and beam loss. These results clearly imply the bias voltage, beam pipe size and focusing solenoids strength were insufficient to cleanly transport the beam to the dump.

Note the QE variation observed at low laser pulse energy. The measured QE is significantly higher for the 200 A

magnet setting suggesting that higher beam magnetization helps to extract more charge by mitigating the space charge effect, but this advantage is lost for higher pulse energies.

### Drift Emittance

The term "drift emittance" refers to the additional emittance growth due to the angular momentum of the electrons generated inside a magnetic field. The drift emittance of magnetized beam with low bunch charge was characterized by measurement and simulation for different laser spot sizes (0.44 and 0.9 mm, respectively) as a function of varying magnetic field on cathode. The results (Fig. 4) for 20 femto-Coulomb bunches from the photogun biased at -200 kV showed encouraging agreement with the GPT simulations. Further details on drift emittance modeling is included in ref [12]. With the increase in laser spot size, an unwanted beam loss was observed at higher end of applied magnetic field on cathode due to the strong focusing effect and large drift emittance.
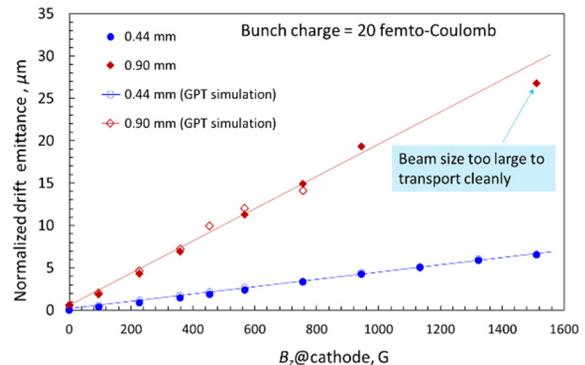
Figure 4: Measured and GPT simulation results of drift emittance versus cathode solenoid field for two laser spot sizes.

### CONCLUSION

A high current, high charge magnetized electron line was developed for fast and efficient cooling of ion beams for JLEIC. Sustained high average current magnetized beam up to 28 mA was demonstrated. High bunch charge magnetized beams up to 0.7 nC at 50kHz repetition rate were also successfully generated, though clearly space charge limited and with significant beam loss. Beam characterization studies were performed under various parameters. To meet the ultimate requirements of the JLEIC cooler design, future tests include beam delivery at average current over 60 mA by installing a new HV power supply, and simulations will be performed to improve beam delivery at nC level.

### ACKNOWLEDGMENTS

# REFERENCES

[1] A. Accardi *et al.*, "Electron-Ion Collider: The next QCD frontier", arXiv:1212.1701, 2012.

[2] A. Shemyakin, and L. R. Prost, "The Recycler Electron Cooler", 2013.

[3] Ya. S. Derbenev, *Nucl. Instr. and Meth. A*, vol. 441, no. 223, 2000.

[4] P. Piot *et al.*, Generation and Dynamics of Magnetized Electron Beams for High-energy Electron Cooling, FERMILAB-CONF-14-142-APC

[5] M. A. Mamun *et al.*, *J. Vac. Sci. Technol. A*, vol. 34, p. 021509, 2016.
doi: 10.1116/1.4939563

[6] C. Hernandez-Garcia *et al.*, *IEEE Trans. Diel. Elec. Insul.*, vol. 23, no. 1, pp. 418-427, Feb. 2016.

[7] C. Hernandez-Garcia *et al.*, *Review of Scientific Instruments*, vol. 88, p. 093303, 2017.

[8] J. Grames *et al.*, "A Biased Anode to Suppress Ion Back-Bombardment in a DC High Voltage Photoelectron Gun", 2008 AIP Conf. Proc. 980 110.

[9] M. Bastaninejad *et al.*, *Nucl. Instr. and Meth. A*, vol. 762, no. 135, 2014.

[10] S. A. K. Wijethunga *et al.*, "Simulation Study of the Magnetized Electron Beam", in *Proc. 9th Int. Particle Accelerator Conf. (IPAC'18)*, Vancouver, Canada, Apr.-May 2018, pp. 3395-3397.
doi:10.18429/JACoW-IPAC2018-THPAK071

[11] M. A. Mamun *et al.*, "Production of Magnetized Electron Beam from a DC High Voltage Photogun", in *Proc. 9th Int. Particle Accelerator Conf. (IPAC'18)*, Vancouver, Canada, Apr.-May 2018, pp. 4567-4570.
doi:10.18429/JACoW-IPAC2018-THPMK108

[12] S. A. K. Wijethunga *et al.*, "Simulation Study of the Emittance Measurements in Magnetized Electron Beam", presented at the 10th Int. Particle Accelerator Conf. (IPAC'19), Melbourne, Australia, May 2019, paper MOPRB110, this conference.